Effect of charge transfer on the geometric structure of a C_{70} monolayer on the surface of Ag(111)

Peng Wang, Han-Jie Zhang, Yan-Jun Li, Chun-Qi Sheng, Ying Shen, Hai-Yang Li, Shi-Ning Bao, and Hong-Nian Li*
Department of Physics, Zhejiang University, Hangzhou 310027, P. R. China
(Received 7 February 2012; revised manuscript received 21 April 2012; published 24 May 2012)

Using scanning tunneling microscopy, we have investigated the adsorption geometry of a C_{70} monolayer on the surface of Ag(111). C_{70} molecules form the commensurate $(\sqrt{13} \times \sqrt{13})R \pm 13.9^\circ$ structure and present temperature-dependent bright/dim contrast. Our analyses reveal that the Coulomb repulsion between the charged molecules is the reason for the pits formed at various fullerene/metal interfaces. For the C_{70} monolayer, the Coulomb repulsion still makes the upright molecular orientation preferable and leads to the invalidation of the rule of lattice match.

DOI: 10.1103/PhysRevB.85.205445 PACS number(s): 68.55.ap, 68.35.Ct, 68.37.Ef, 68.43.Hn

I. INTRODUCTION

It is general knowledge that the geometric and electronic structures of an adsorbate-substrate system are closely related to each other. For fullerene overlayer on metal surface, studies in recent years[1–4] revealed that the geometry had remarkable effects on the electronic structure. C_{60} can dig pits on metal surfaces, and the pits effectively facilitate charge transfer from metal to C_{60}. Logically, charge transfer should play a role in determining the geometric structure, because the charged fullerenes alter intermolecular and molecule-metal interactions. However, researchers have not paid sufficient attention to the effect of charge transfer up to this date. In this paper we report a scanning tunneling microscopy (STM) study of C_{70} overlayer on the surface of Ag(111) aimed at the observation of the effect of charge transfer. The reasons for selecting the C_{70}/Ag(111) system are as follows. First, this system exhibits a large amount of charge transfer (>2.6 e per molecule).[5] Second, the lowest unoccupied molecular orbital (LUMO) distributes mainly around the poles of the ellipsoidal-shaped C_{70} molecule,[6] which may induce more observable effects of charge transfer.

The effect of charge transfer on the geometric structure should be intricate. It would be helpful to briefly survey the achievements made in the past years about the geometric structures of C_{60} and C_{70} on the (111) surfaces of the noble metals (Cu, Ag, Au). C_{60} generally forms the first-order commensurate lattices on these surfaces, the (4×4) structure on Cu(111),[7] and the $(2\sqrt{3} \times 2\sqrt{3})R30^\circ$ structure on Ag or Au(111).[8,9] Some higher-order commensurate structures only exist as metastable states for the samples not subjected to annealing at sufficiently high temperatures[10–13] or exist due to the confinement of the substrate steps.[14] C_{70} also forms the (4×4) structure on Cu(111).[15] These observations have been understood in the literature by the rule of lattice match. For C_{60}, the nearest-neighbor distance (NND) in the (111) plane of the face-centered-cubic (fcc) crystal is 1.002 nm.[16] Accordingly, the (4×4) structure is the stable phase for C_{60} on Cu(111) with a lattice mismatch of only ~2.0%, and the $(2\sqrt{3} \times 2\sqrt{3})R30^\circ$ structure is the stable phase for C_{60} on Ag or Au(111) with almost perfect lattice match [the atomic distance is 0.256, 0.289, and 0.288 nm for Cu(111), Ag(111), and Au(111) surfaces, respectively].[17] For a C_{70} solid, the NND is dependent on the molecular orientations: 1.06 nm for the freely rotating molecules [the high-temperature fcc and hexagonal close-packed (hcp) structures][18] and 1.01 nm (near that of C_{60} solid) for the molecules aligning their long axes parallel to each other and perpendicular to the close-packed crystal plane (the deformed hcp structure).[18] C_{70} molecules adopt the upright orientation (with the long axis parallel to sample normal)[15] on the surface of Cu(111), and thus the stable phase is the observed (4×4) structure. The most stable phases of C_{70} monolayers (MLs) on the surfaces of Ag(111) and Au(111) have, to the best of our knowledge, not been reported so far. There have been only a few STM measurements on not well-defined C_{70}/Ag(111) and C_{70}/Au(111) samples in air condition[19–21] or in liquids.[22,23] Following the rule of lattice match, we may expect the $(2\sqrt{3} \times 2\sqrt{3})R30^\circ$ structure as being the stable phase if the molecules take the upright orientation. This expectation will be tested in the present work for C_{70}/Ag(111).

Another important achievement is the discovery of the pits formed at the interfaces, as mentioned previously.[1–4] There are two types of pit configurations at the interfaces between C_{60} and the (111) surfaces of the noble metals: the one-atom vacancy for Ag(Au)[11,24] and the seven-atom vacancy for Cu.[1] The preferred pit configuration for one specific substrate has most recently got an interpretation in terms of the substrate geometric structure.[25] However, a fundamental question needs to be answered: Why do the pits form (either in a one- or seven-atom vacancy)? Our work indicates that the Coulomb repulsion between the charged molecules is the reason for the pit formation.

II. EXPERIMENT

Experiments were performed in an Omicron instrument for surface science with a base pressure better than 2.0×10^{-10} mbar. The clean and ordered surface of an Ag(111) single crystal was obtained by a standard Ar^+ sputtering and annealing procedure. Low-energy electron diffraction was used to determine the crystallographic directions of the surface. Thoroughly degassed small C_{70} single crystals were sublimed from a Ta boat located at about 11 cm from the Ag(111) substrate. The sample was kept at room temperature during C_{70} deposition. We first prepared a C_{70} overlayer of ~0.9 ML. The coverage is the average of many large areas of the sample. Then we grew a C_{70} multilayer of ~4.5 ML thickness. Annealing the multilayer at 300 °C with a duration

of 20 min resulted in a well-ordered ML [1 ML C_{70}/Ag(111)]. The ML sample was further annealed at 380 °C and 500 °C for 20 min to study the structural evolution. STM images were recorded at room temperature for every stage of the sample preparation history. The images were measured in constant current mode using a chemically etched tungsten tip, and the biases were referred to the sample.

III. RESULTS AND DISCUSSION

Growth of C_{70} film on the Ag(111) is not layer-by-layer, at least for the first few layers. Figure 1(a) shows a 200 × 200 nm image of the nominal 0.9 ML sample. Many patches of the second-layer and an island of the third-layer molecules can be seen with large areas of bare Ag(111). The line profiles in Fig. 1(b) exhibit that the height of the first molecular layer (∼0.53 nm) is obviously less than those of the second and third layers (∼0.78 nm). The height difference indicates pits formed at the C_{70}/Ag(111) interface, which will be discussed in detail later.

Figure 2 shows the representative molecular-resolved STM images of the samples. Figure 2(a) was acquired on the first molecular layer of the 0.9 ML sample. Figure 2(b) is for the 1 ML C_{70}/Ag(111) prepared by annealing at 300 °C, and Fig. 2(c) is for the sample annealed at 380 °C. The annealing at 500 °C desorbed all molecules on the terraces, and the STM image is not shown here. From Fig. 2, C_{70} molecules form in-plane close-packed hexagonal lattice and exhibit out-of-plane bright/dim (B/D) contrast (the difference in the apparent height of the molecules).

To deduce the lattice structure, we show an image in Fig. 3(a) that was successively measured in the same region as Fig. 2(b) with a time interval of 4 min. The close-packed lattice is indicated by a hexagon in Fig. 3(a). Profile analyses revealed that the NND of the molecules is 1.06 ± 0.02 nm along the direction of the upper or lower sides of the hexagon. The NND along other sides of the hexagon is 1.04 ± 0.02 nm [Fig. 3(b)]. By comparing Fig. 3(a) with Fig. 2(b), slight thermal drift in the horizontal direction can be seen. Taking into consideration the thermal drift, the NND of the C_{70} lattice should be the same and near 1.04 nm for the molecular chains in all directions. The rotational angle of the lattice is +14° with respect to the [$\bar{1}$01] direction of the Ag(111).

On the basis of the NND and the rotational angle, we conclude that the C_{70} lattice is the first-order commensurate

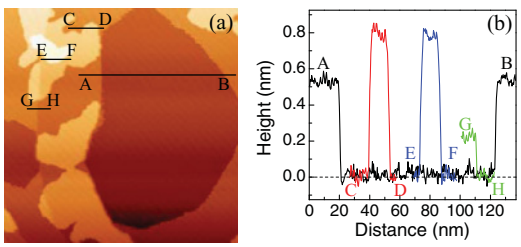

FIG. 1. (Color online) (a) STM image (200 × 200 nm, V = 1.0 V, I = 0.3 nA) of a 0.9-ML C_{70} film on the surface of Ag(111). (b) Line profiles indicating the heights of the first molecular layer (AB), the second molecular layer (CD), the third molecular layer (EF), and the atomic step of the Ag(111) (GH).

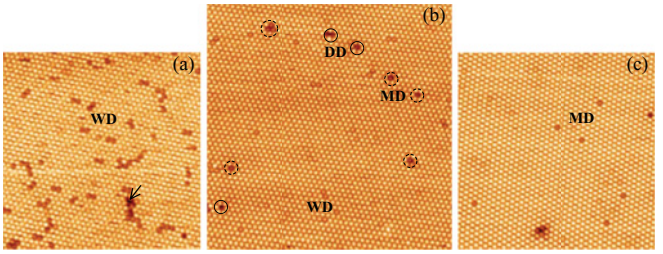

FIG. 2. (Color online) Molecular-resolved STM images of (a) the 0.9 ML sample (40 × 40 nm, V = −0.75 V, I = 0.3 nA), (b) the ML sample annealed at 300 °C (50 × 50 nm, V = 0.76 V, I = 0.04 nA), and (c) the sample annealed at 380 °C (40 × 40 nm, V = −0.41 V, I = 0.23 nA). The arrow in (a) indicates a molecular vacancy rather than a deeper molecule. The DD and MD molecules in (b) are highlighted with solid and dashed circles, respectively.

$(\sqrt{13} \times \sqrt{13})R \pm 13.9°$ structure. The model of the $(\sqrt{13} \times \sqrt{13})R + 13.9°$ structure is illustrated in Fig. 4(a). The close-packed molecular chain aligns along the [$\bar{3}\bar{1}$4] direction of the substrate, and the molecules adsorb equivalently at the atop sites with the NND of $\sqrt{13}a = 1.042$ nm [a is the atomic distance in the Ag(111) surface]. The angle between the [$\bar{3}\bar{1}$4] and the [$\bar{1}$01] direction is 13.9°. According to Fig. 4(a), C_{70} molecules can also align along the [$\bar{4}$13] direction to form the $(\sqrt{13} \times \sqrt{13})R - 13.9°$ structure that is actually identical to the $(\sqrt{13} \times \sqrt{13})R + 13.9°$ structure based on the symmetry. This is indeed the case. We observed the $(\sqrt{13} \times \sqrt{13})R - 13.9°$ structure in other regions of the sample and showed the $(\sqrt{13} \times \sqrt{13})R - 13.9°$ structure in Fig. 2(c) as the representative image of another sample. Except for the $(\sqrt{13} \times \sqrt{13})R \pm 13.9°$ structure, we did not find any other structures by the STM measurements in a great many regions of the samples of Figs. 2(b) and 2(c). For the 0.9 ML sample, we did not measure as many images as for the other two samples. However, as far as the measured regions are concerned, no other structure was found.

In Figs. 2(b), 2(c), and 3(a) the overwhelming majority of the C_{70} molecules take the upright orientation, since they exhibit round shape. The inset of Fig. 3(a) enlarges the framed part to show the comparison of the predominant round-shaped molecules with few ellipsoidal-shaped (lying-down or tilted orientations) molecules, which manifests that the resolution of our measurements is good enough to assure the conclusion of

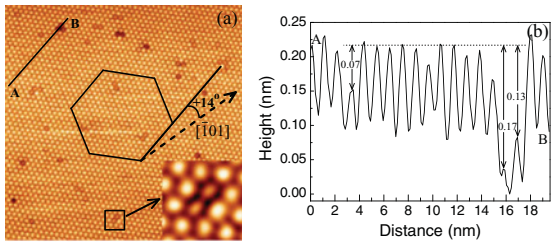

FIG. 3. (Color online) (a) Indication of the close-packing and the rotational angle of the C_{70} lattice. The image (50 × 50 nm, V = 0.76 V, I = 0.04 nA) was successively measured in the same region as Fig. 2(b). The inset enlarges the framed part. (b) A line profile along AB showing the height differences between the B molecules and the three types (WD, MD, and DD) of D molecules.

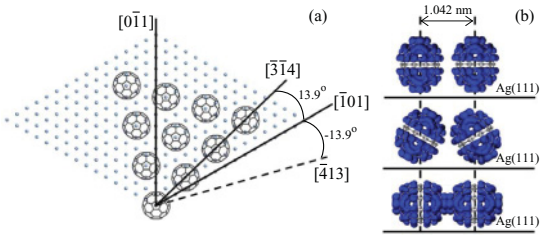

FIG. 4. (Color online) (a) Model of the $(\sqrt{13} \times \sqrt{13})R \pm 13.9°$ structure. The Ag atoms are assumed to be located at their unreconstructed sites, and the C_{70} molecules take the upright orientation. (b) Molecular orbitals (the superposition of the LUMO and LUMO + 1) illustrating the preferable upright orientation of the C_{70} molecules. The separation and size of the molecules are proportional to actual values.

the upright orientation for most C_{70} molecules. However, the C_{70} molecules do not form the $(2\sqrt{3} \times 2\sqrt{3})R30°$ structure as expected on the basis of lattice match. Considering the perfect (unreconstructed) surface of the Ag(111) before C_{70} adsorption and the sample having been annealed up to 380 °C in ultrahigh vacuum, the $(\sqrt{13} \times \sqrt{13})R \pm 13.9°$ structure of the 1 ML C_{70}/Ag(111) indicates a new mechanism of the adsorption geometry for fullerene/metal interfaces. We suggest that the new mechanism is the effect of charge transfer from metal substrate to fullerene, which was neglected in the rule of lattice match. Considering the fact that the electrostatic interaction between the inhomogeneous electron density of neutral C_{70} molecules plays an important role in the crystal structures of bulk C_{70},[18] it becomes understandable that the enhanced Coulomb repulsion between the charged (>2.6 e) C_{70} molecules expands the lattice by a NND increment of 0.041 (=1.042 − 1.001) nm from the $(2\sqrt{3} \times 2\sqrt{3})R30°$ to the $(\sqrt{13} \times \sqrt{13})R \pm 13.9°$ structure. The suggestion of the effect of charge transfer will be further supported by the study of the B/D contrast in the following.

Different from the unchanged lattice structure, the B/D contrast presents strong dependence on annealing. In Fig. 2(a) all D molecules have height smaller than that of the B molecules by 0.05–0.08 nm, and we refer to these D molecules as WD (weak dim). After annealing at 300 °C [Figs. 2(b) and 3(a)], the number of WD molecules decreases distinctly, but deeper molecules arise. Some molecules are lower than the B molecules by 0.10–0.13 nm, which are labeled with MD (middle dim). There are few molecules lower than the B molecules by 0.17–0.19 nm, and we label them with DD (dark dim). After further annealing at 380 °C, the WD and DD molecules disappear in Fig. 2(c).

The large height difference between the DD and B molecules can only be explained with the pits formed at the C_{70}/Ag(111) interface. What's more, there are two types of pits because even the B molecules are sited inside pits. The pits beneath the B molecules are evidenced by the height difference [0.25 nm, greater than the atomic step of the Ag(111) substrate] between the first and the second molecular layer in Fig. 1. The height difference was also observed for C_{60} on Au(111) and Cu(111) surfaces in some early works[7,14] and was initially interpreted in terms of electronic states or molecular orientations. However, subsequent works[2,10] revealed that the height difference was simply induced by the pits beneath the first-layer molecules. By inspection of Fig. 4(a) we can reasonably speculate that the two types of pits at the C_{70}/Ag(111) interface are also the seven-atom and one-atom vacancies, as observed on 1 ML C_{60}/Cu(111)[1] and 1 ML C_{60}/Ag(Au)(111),[11,24] respectively. The former corresponds to the case of the seven Ag atoms beneath the C_{70} molecule that were removed, and the latter corresponds to the Ag atom just beneath the five-membered carbon ring that was removed. The molecular orientation should be another origin of the B/D contrast. C_{70} has an ellipsoidal shape with the long and the short axes of 0.798 nm and 0.715 nm, respectively.[26] Different molecular orientations would lead to visible height differences up to 0.083 nm. The possibility of C_{60} impurity was excluded by the observation that some molecules switched from MD to DD or from DD to MD during successive scanning.

In terms of the pits and the molecular orientations, the temperature-dependent B/D contrast of the 1 ML C_{70}/Ag(111) can be interpreted as follows. The as-deposited C_{70} molecules dig the one-atom pits on the surface of Ag(111). The B features in Fig. 2(a) are those upright molecules, while the WD features are the lying-down or tilting molecules. After annealing at 300 °C, more molecules take the upright orientation, so the number of WD molecules decreases. Meanwhile, some molecules dig the seven-atom pits. The MD and DD features in Fig. 2(b) correspond to the molecules in the seven-atom pits with different molecular orientations. The MD molecules are upright or near upright, while the DD molecules are lying-down or near lying-down. According to a density functional theory calculation,[27] the seven-atom and one-atom pits on the Au(111) surface (Au has nearly identical lattice constant as Ag) can result in a height difference of 0.165 nm. Then the DD molecules can have a height smaller than the B molecules by an amount of up to 0.248 (=0.165 + 0.083) nm. Of course, the measured height difference should be smaller than 0.248 nm for an isolated DD molecule embedded in surrounding higher molecules [the case of Fig. 2(b)]. So the observed B/DD height difference is 0.17–0.19 nm. The height of the MD molecules can be understood analogously. When the sample was annealed at higher temperature (380 °C), more and more molecules take the upright orientation, and thus the WD and DD features disappear. The small scattering (<0.03 nm) of the height for the MD molecules in Fig. 2(c) may be due to few molecules still tilting somewhat in the seven-atom pits.

The previous interpretation of the B/D contrast is self-consistent. However, two fundamental questions remain. First, why is the upright orientation preferable? Second, why do the pits form? These questions must be answered to get a thorough understanding of the fullerene/metal interfaces [not merely the C_{70}/Ag(111) interface]. Prompted by the suggestion of the effect of charge transfer in explaining the $(\sqrt{13} \times \sqrt{13})R \pm 13.9°$ structure, we think that the Coulomb repulsion between the charged molecules is the reason for the upright orientation. The LUMO orbital distributes near the poles of C_{70},[6] as illustrated in Fig. 4(b), for two adjacent molecules with different relative orientations. Since the electrons could occupy both the twofold degenerated LUMO and the nondegenerated LUMO + 1,[5] we plot in Fig. 4(b) the superposition of the

three orbitals (calculated with the CASTEP package, for detail see Ref. 5). With the intermolecular distance of 1.042 nm, it is impossible for two adjacent C_{70} molecules to take the lying-down orientation along a line on the Ag(111) surface [the bottom of Fig. 4(b)], since the Coulomb repulsion would be too large due to the intersecting of the electron distribution near the poles of the molecules. On the contrary, the upright orientation [the top of Fig. 4(b)] can effectively minimize the Coulomb interaction. Before thermodynamic equilibrium, dispersed lying-down molecules or a few adjacent-tilting molecules are possible but with high stress energy of the C_{70} lattice. This is the case of the WD molecules in Fig. 2(a). The stress energy can be released by two manners upon annealing. First, the molecules adjust their orientations from lying-down or tilting to upright. Second, the molecules dig deeper pits. The first manner is reflected in Figs. 2(b) and 2(c) by the substantially decreased number of D molecules. The emergence of the MD and DD molecules in Fig. 2(b) is the reflection of the second manner.

On the basis of a quantitative estimate of the interaction between two charged C_{70} molecules, we suggest that the Coulomb repulsion is also the reason for the pit formation. Before calculating the interaction, we mention that Ref. 5 only reported the low limit (2.6 e) of the amount of charge transfer for the 1 ML C_{70}/Ag(111). For the purpose of the present work, we reanalyzed the experimental data (x-ray absorption spectra and photoemission spectra) of Ref. 5 and found that the amount of charge transfer should be no more than 2.9 e. According to Fig. 4(b), the extra 2.6–2.9 electrons [transferred from the Ag(111)] distribute on the surfaces of two semispheres separated by the 10 C atoms around the equator of the ellipsoidal-shaped C_{70} molecule. If we assume that the electron distribution on the semisphere surfaces is homogeneous, a C_{70} ion can be replaced by two point charges in calculating intermolecular electrostatic interaction. Each point charge ($q = 1.3$–1.45 e) locates at the long axis with a distance of 0.1775 nm from one of the two poles of C_{70}. The distance of 0.1775 nm is half the radium (0.355 nm)[28] of C_{60} because the two semispheres of C_{70} just form a C_{60} molecule. The electrostatic interaction for the two C_{70} ions in the top of Fig. 4(b) can thus be calculated with the formula $\frac{2}{4\pi\varepsilon_0} \times \frac{q^2}{R} + \frac{2}{4\pi\varepsilon_0} \times \frac{q^2}{R'}$, where R is the distance between the centers of the molecules and R' the distance between the two point charges in the upper semisphere of one molecule and the lower semisphere of another molecule, respectively. With the values of 1.042 nm for R and 1.132 nm for R', the estimated Coulomb repulsion is within the range from 8.96 eV (for $q = 1.3$ e) to 11.15 eV (for $q = 1.45$ e). Although the previous model is very simple and has some crude approximations, we can at least say that the Coulomb repulsion is substantially larger than the heat of sublimation of $\sim$1.95 eV[29] per molecule for C_{70} crystal. The two-dimensional C_{70} lattice would definitely collapse if there is no compensating factor.

We then consider the possible compensating factors. The image charges in the metal side, if existing, should help to stabilize the C_{70} lattice. The existence of image charges in some cases, such as a photoelectron escaping from a metal surface, is the requirement to meet the boundary condition (the electric field must be perpendicular to metal surface). In the case of the present work, however, the charged C_{70} molecules intimately combine with the substrate with good electric contact. There might be no image charge, or at least the possible small amount of image charges does not play a crucial role. The Madelung effect, which is the most important factor to stabilize bulk ionic crystals, may play a role. However, for the interface system studied here, it is difficult to specify where the LUMO and LUMO + 1 electrons of the C_{70} ions are from. The electrons may be partially from the Ag atoms in direct contact with C_{70} and may also be from the whole Ag single crystal. We believe that the Ag atoms in direct contact with C_{70} are positively charged and present some Madelung effect (attract the negatively charged C_{70} ions), but the effect should be less significant than the cases of bulk ionic crystals. Besides, the Madelung effect and the possible image charges of an unreconstructed substrate stabilize the C_{70} lattice only in the direction normal to the surface. They cannot hinder the in-plane collapse caused by the strong intermolecular Coulomb repulsion. Therefore, the pits must form as the unique factor to prevent the in-plane collapse. In other words the intermolecular Coulomb repulsion is the reason for the pits observed on the 1 ML C_{70}/Ag(111).

Our suggestion of the Coulomb repulsion provides a unified interpretation of the pits observed for 1 ML $C_{60}(C_{70})$/Cu(Ag,Au)(111). For the case of the 1 ML C_{60}/Cu(111),[1] the Coulomb repulsion between two adjacent C_{60}^{3-} ions with a separation of $R = 1.02$ nm is calculated to be $\sim$12.7 eV ($=\frac{1}{4\pi\varepsilon_0} \times \frac{(3e)^2}{R}$, since a C_{60} ion can be replaced by a point charge at the molecular center due to the delocalized property of the LUMO and the very near spherical symmetry of the molecule), which is greatly larger than the heat of sublimation of $\sim$1.65 eV per molecule for C_{60} crystal.[29] Therefore, the seven-atom pit[1] must form to stabilize the heavily charged C_{60} overlayer. For C_{60} MLs on the surfaces of Ag(111) and Au(111), the amount of charge transfer is 0.7–0.75 e[30,31] and 0.8 e,[32] respectively, and the Coulomb repulsion is relatively small but still comparable with the heat of sublimation. The seven-atom pit may be unnecessary, but the one-atom pit is needed to stabilize the lattices. The Coulomb repulsion for the 1 ML C_{70}/Ag(111) is in between the cases of 1 ML C_{60}/Cu(111) and 1 ML C_{60}/Ag(Au)(111). So the two types of pits coexist in Figs. 2(b) and 2(c).

At the conclusion of this paper we mention that annealing plays a role in the pit formation. The observation of only one-atom pits in Fig. 2(a) indicates the assistance of annealing to the formation of the deeper (seven-atom) pits. The annealing can facilitate the pit formation by providing energy to overcome some barriers and by increasing the amount of charge transfer. However, it is the Coulomb repulsion that ultimately determines the formation of the pits.

IV. CONCLUSION

In summary, the Coulomb repulsion between the charged molecules helps C_{70} to form the $(\sqrt{13} \times \sqrt{13})R \pm 13.9^\circ$ lattice on the surface of Ag(111) rather than the $(2\sqrt{3} \times 2\sqrt{3})R30^\circ$ structure expected on the basis of lattice match.

The Coulomb repulsion determines the upright orientation of the C_{70} molecules. More importantly, the Coulomb repulsion is the reason for the pits formed at the various fullerene/metal interfaces.

ACKNOWLEDGMENTS

This work is supported by the National Natural Science Foundation of China under Grant No. 11079028 and the Fundamental Research Funds for the Central Universities.

*Corresponding author: phylihn@public.zju.edu.cn

[1]W. W. Pai, H. T. Jeng, C.-M. Cheng, C.-H. Lin, X. D. Xiao, A. D. Zhao, X. Q. Zhang, G. Xu, X. Q. Shi, M. A. Van Hove, C.-S. Hsue, and K.-D. Tsuei, Phys. Rev. Lett. **104**, 036103 (2010).

[2]J. A. Gardener, G. A. D. Briggs, and M. R. Castell, Phys. Rev. B **80**, 235434 (2009).

[3]X. Q. Zhang, W. He, A. D. Zhao, H. N. Li, L. Chen, W. W. Pai, J. G. Hou, M. M. T. Loy, J. L. Yang, and X. D. Xiao, Phys. Rev. B **75**, 235444 (2007).

[4]C. Silien, N. A. Pradhan, W. Ho, and P. A. Thiry, Phys. Rev. B **69**, 115434 (2004).

[5]P. Wang, L. Meng, X.-B. Wang, Y.-J. Li, C.-Q. Sheng, J.-O. Wang, H.-J. Qian, K. Ibrahim, and H.-N. Li, J. Phys.: Condens. Matter **23**, 395002 (2011).

[6]X.-B. Wang, H.-K. Woo, X. Huang, M. M. Kappes, and L.-S. Wang, Phys. Rev. Lett. **96**, 143002 (2006).

[7]T. Hashizume, K. Motai, X. D. Wang, H. Shinohara, Y. Saito, Y. Maruyama, K. Ohno, Y. Kawazoe, Y. Nishina, H. W. Pickering, Y. Kuk, and T. Sakurai, Phys. Rev. Lett. **71**, 2959 (1993).

[8]E. I. Altman and R. J. Colton, Surf. Sci. **295**, 13 (1993).

[9]E. I. Altman and R. J. Colton, Phys. Rev. B **48**, 18244 (1993).

[10]W. W. Pai, C.-L. Hsu, M. C. Lin, K. C. Lin, and T. B. Tang, Phys. Rev. B **69**, 125405 (2004).

[11]L. Tang, Y. Xie, and Q. Guo, J. Chem. Phys. **135**, 114702 (2011).

[12]G. Schull and R. Berndt, Phys. Rev. Lett. **99**, 226105 (2007).

[13]T. Hashizume and T. Sakurai, Surf. Rev. Lett. **3**, 905 (1996).

[14]E. I. Altman and R. J. Colton, Surf. Sci. **279**, 49 (1992).

[15]X.-D. Wang, V. Y. Yurov, T. Hashizume, H. Shinohara, and T. Sakurai, Phys. Rev. B **49**, 14746 (1994).

[16]P. A. Heiney, J. E. Fischer, A. R. McGhie, W. J. Romanow, A. M. Denenstein, J. P. McCauley Jr., A. B. Smith III, and D. E. Cox, Phys. Rev. Lett. **66**, 2911(1991).

[17]D. R. Lide, *CRC Handbook of Chemistry and Physics*, 87th ed. (Taylor and Francis, Boca, Raton, Florida, 2007).

[18]M. A. Verheijen, H. Meekes, G. Meijer, P. Bennema, J. L. de Boer, S. van Smaalen, G. van Tendeloo, S. Amelinckx, S. Muto, and J. van Landuyt, Chem. Phys. **166**, 287 (1992).

[19]H. N. Aiyer, A. Govindaraj, and C. N. R. Rao, Philos. Mag. Lett. **72**, 185 (1995).

[20]Y. Zhang, X. Cao, and M. J. Weaver, J. Phys. Chem. **96**, 510 (1992).

[21]S. Guo, D. Fogarty, P. Nagel, and S. A. Kandel, Proc. SPIE **5513**, 185 (2004).

[22]N. Katsonis, A. Marchenko, and D. Fichou, Adv. Mater. **16**, 309 (2004).

[23]A. L. Deering and S. A. Kandel, Langmuir **22**, 10025 (2006).

[24]H. I. Li, K. Pussi, K. J. Hanna, L.-L. Wang, D. D. Johnson, H.-P. Cheng, H. Shin, S. Curtarolo, W. Moritz, J. A. Smerdon, R. McGrath, and R. D. Diehl, Phys. Rev. Lett. **103**, 056101 (2009).

[25]X.-Q. Shi, M. A. Van Hove, and R.-Q. Zhang, Phys. Rev. B **85**, 075421 (2012).

[26]S. J. Woo, E. Kim, and Y. H. Lee, Phys. Rev. B **47**, 6721 (1993).

[27]L. Tang, X. Zhang, Q. Guo, Y.-N. Wu, L.-L. Wang, and H.-P. Cheng, Phys. Rev. B **82**, 125414 (2010).

[28]R. D. Johnson, D. S. Bethune, and C. S. Yannoni, Acc. Chem. Res. **25**, 169 (1992).

[29]J. Abrefah, D. R. Olander, M. Balooch, and W. J. Siekhaus, Appl. Phys. Lett. **60**, 1313 (1992).

[30]L. H. Tjeng, R. Hesper, A. C. L. Heessels, A. Heeres, H. T. Jonkman, and G. A. Sawatzky, Solid State Commun. **103**, 31 (1997).

[31]W. L. Yang, V. Brouet, X. J. Zhou, H. J. Choi, S. G. Louie, M. L. Cohen, S. A. Kellar, P. V. Bogdanov, A. Lanzara, A. Goldoni, F. Parmigiani, Z. Hussain, and Z.-X. Shen, Science **300**, 303 (2003).

[32]C. T. Tzeng, W. S. Lo, J. Y. Yuh, R. Y. Chu, and K. D. Tsuei, Phys. Rev. B **61**, 2263 (2000).